Quantum Simulator

DOI: 10.1002/ange.201301435

Hexamethoxyphenalenyl as a Possible Quantum Spin Simulator: An Electronically Stabilized Neutral π Radical with Novel Quantum Coherence Owing to Extremely High Nuclear Spin Degeneracy**

Akira Ueda, Shuichi Suzuki, Kenta Yoshida, Kozo Fukui, Kazunobu Sato, Takeji Takui, Kazuhiro Nakasuji, and Yasushi Morita**

In recent years, organic open-shell molecules have drawn increasing attention from both fundamental and applied aspects, because they show unique structural electronic features and spin-nature-based functionalities that are intrinsically different from closed-shell molecules.[1–4] The latest trends are exemplified in chemical entities affording dynamic nuclear polarization to give rise to enormous sensitivity enhancement in biological NMR spectroscopy[3] and the use of molecular electron spins as synthetic spin quantum bits (qubits) for quantum information science and quantum computers (QCs).[4] The latest progress in molecular spin science has been underlain by the design and synthesis of air-stable organic open-shell molecules.[1]

Phenalenyl (PLY in Scheme 1) is an odd-alternant carbon-centered neutral π radical with a high thermodynamic stability arising from delocalization of an unpaired electron over the planar D_{3h}-symmetric 13π-electron system. However, owing to a kinetic instability, in solution, PLY gradually decomposes to peropyrene, a closed-shell polycyclic hydrocarbon, through σ dimerization even under oxygen-free conditions.[5] Introduction of *tert*-butyl groups into the phenalenyl skeleton allowed us to isolate, for the first time, TBPLY (Scheme 1) in its crystalline state.[6] Since then, by using the steric protection effect of bulky substituents, several kinds of air-stable phenalenyl derivatives were synthesized and isolated, all of which have exotic structures and properties owing to the extensively spin-delocalized nature of the phenalenyl system.[7–9] Efforts have been made to synthesize electronically stabilized phenalenyl systems by introducing heteroatom functional groups, such as alkoxy,[10a–c,11a] amino,[10b–d] thio,[11] and cyano[10a,12] substituents at the peripheral carbon atoms. These phenalenyl radicals are important to understand electronic perturbation effects and intermolecular interactions attributable to the introduced heteroatom substituents in solids. However, detailed investigations in this context, particularly relevant to the electronic-spin properties, have rarely been reported except for thio- or cyano-substituted radicals,[11a,12] owing to the intrinsic kinetic instability of the neutral radical species.[13]

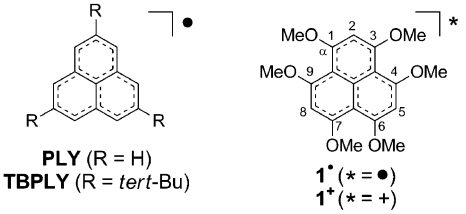

Scheme 1. Structures of PLY, TBPLY, **1**•, and **1**$^+$.

Here we report the synthesis, electronic-spin structure, and novel spin-based quantum coherence of the hexamethoxylphenalenyl neutral π radical **1**• (Scheme 1), in which the coherence is related to a large number of equivalent nuclear spins. Interestingly, the symmetrical introduction of six methoxy groups into the phenalenyl skeleton played a crucial role not only to electronically stabilize the radical species **1**• by the resonance effect,[14] but also to provide extremely well-resolved ESR hyperfine splittings with a very small linewidth in solution associated with temperature-dependent dynamic behavior of spin angular momenta in molecular frames. This unique hyperfine spectroscopic feature allowed us to investigate spin-based quantum nature owing to the extremely high nuclear spin degeneracy by using time-domain ESR spectroscopy. We demonstrate the appearance of novel quantum coherence in **1**• in quest of molecular quantum spin simulators, which can afford analog computational tools enabling us to simulate formidable quantum properties, such as spin dynamics arising from a large number of interacting equivalent nuclear spins.

The synthesis of the neutral radical **1**• was accomplished by chemical reduction of the cation salt **1**$^+$·BPh_4^-[15] with an excess of sodium in THF under oxygen- and moisture-free

[*] Dr. A. Ueda, Dr. S. Suzuki, K. Yoshida, Dr. K. Fukui, Prof. Dr. K. Nakasuji, Prof. Dr. Y. Morita
Department of Chemistry, Graduate School of Science
Osaka University
Toyonaka, Osaka 560-0043 (Japan)
E-mail: morita@chem.sci.osaka-u.ac.jp
Homepage: http://www.chem.sci.osaka-u.ac.jp/lab/nakasuji/morita/index_eng.html
Prof. Dr. K. Sato, Prof. Dr. T. Takui
Department of Chemistry and Molecular Materials Science
Graduate School of Science, Osaka City University
Sumiyoshi-ku, Osaka 558-8585 (Japan)
E-mail: takui@sci.osaka-cu.ac.jp
Homepage: http://www.qcqis.sci.osaka-cu.ac.jp/ms/

[**] This work was partially supported by Grants-in-Aid for Scientific Research on Innovative Areas (No. 20110006 and Quantum Cybernetics), Scientific Research (B) (No.23350011), and Elements Science and Technology Project from Ministry of Education, Culture, Sports, Science and Technology (Japan), and also by Core Research for Evolutional Science and Technology (CREST-JST) and FIRST-Quantum Information Processing Project.

Supporting information for this article is available on the WWW under http://dx.doi.org/10.1002/anie.201301435.

conditions. The neutral radical **1**• was obtained as a blue solid and is stable in both a degassed solution and the solid state under inert gas atmosphere for a few weeks.[16]

To evaluate the electronic-spin structure of **1**• in solution, we have carried out cw-ESR and ^{1}H ENDOR/TRIPLE measurements of **1**• in degassed toluene (6×10^{-4} M) at 298 K (Figure 1). The ESR spectrum gave an extremely well-resolved hyperfine structure with very sharp linewidths

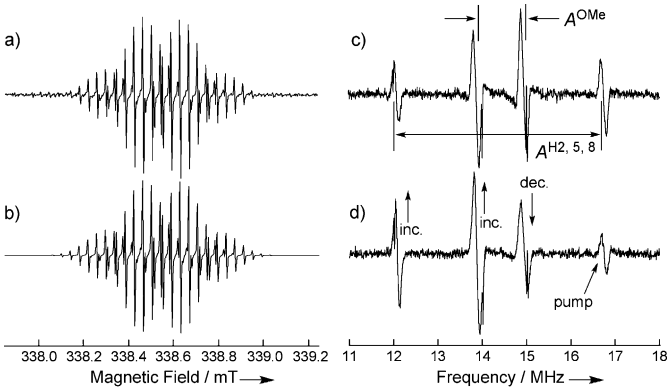

Figure 1. a) Observed ESR spectrum of **1**• in degassed toluene (6×10^{-4} M) at 298 K. The microwave frequency used is 9.483631 GHz and the observed *g* value is 2.0047. The modulation frequency and amplitude used for phase-sensitive detection were 10 kHz and 0.0012 mT, respectively, to avoid side-band production effects. b) Simulated ESR spectrum. The Lorentzian line shape with 0.0038 mT of the maximum-slope-line width for a single transition was used. Any anisotropic contributions to the spectrum are not included in the simulation. c) ^{1}H ENDOR and d) TRIPLE (pump frequency, 16.74 MHz) spectra of **1**• in degassed toluene (6×10^{-4} M) at 298 K.

(Figure 1a). The *g* value is 2.0047 and is significantly larger than that of the parent PLY (2.00265).[5b] The ^{1}H ENDOR spectrum (Figure 1c) reveals that there are only two kinds of hyperfine couplings, which are attributable to protons of the 2-, 5-, and 8-positions of the phenalenyl skeleton and those of the methoxy groups. In addition, their relative signs were unequivocally determined on the basis of the TRIPLE spectrum (Figure 1d). An ESR spectral simulation based on the experimental hyperfine coupling constants (hfccs) satisfactorily reproduced the side-band-free observed ESR spectrum (Figure 1b).

Table S1 in the Supporting Information summarizes the observed (at 298 K) and calculated hfccs of **1**• together with the observed ones of PLY.[5b] The observed hfcc of the protons on the 2-, 5-, and 8-positions ($A^{H2,5,8}$) for **1**• (+0.1662 mT) is in good agreement with the calculated one (+0.2105 mT),[17] thereby demonstrating the occurrence of an extensive spin delocalization over the whole molecular skeleton in a C_3-symmetrical fashion, as illustrated by the calculated spin density distribution (Figure 2a). In contrast, there is a significant difference between the observed (+0.0392 mT) and calculated (+0.0802 mT) hfcc of the methoxy groups A^{OMe} for **1**•. The origin of this difference is discussed later. In addition, we found that the absolute value of the observed $A^{H2,5,8}$ for **1**• (0.1662 mT) is smaller than that for PLY (0.1805 mT), that is, the spin density on the 2-, 5-, and 8-positions of **1**• decreases by

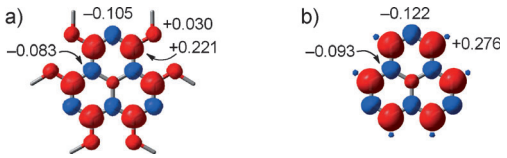

Figure 2. Calculated spin density distribution of a) **1**• and b) PLY. Values represent the calculated spin density on each of the carbon atoms. The calculations were performed at the UB3LYP/DZVP2 level of theory. Red and blue regions denote the positive and negative spin densities, respectively.

comparison with that of PLY (Figure 2). This is because the sizable spin densities of **1**• are delocalized onto the methoxy groups from the phenalenyl skeleton by the electronic resonance effect.[18] Consequently, the spin densities at the 1-, 3-, 4-, 6-, 7-, and 9-carbon atoms (α-carbons) in **1**• significantly decreased from those in PLY (Figure 2). The highly spin-delocalized nature of **1**• induced by the resonance effect of the methoxy groups contributes to the electronic stabilization of the neutral radical **1**•.[14]

To gain further insight into the substituent effect of the methoxy groups on the spin-delocalized nature of **1**•, variable-temperature ESR measurements of **1**• in degassed toluene (6×10^{-4} M) were carried out in the range of 170–300 K (Figure 3 and Figure S6 in the Supporting Information). Both the hyperfine structures and ESR signal intensities of **1**•

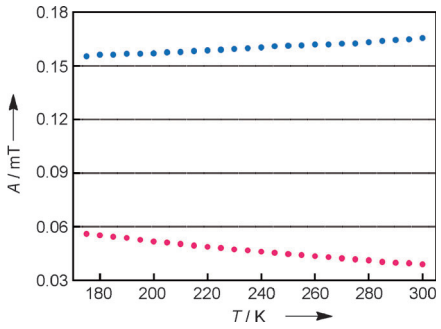

Figure 3. Temperature dependence of $A^{H2,5,8}$ (blue circles) and A^{OMe} (pink circles) of **1**• obtained from the ESR spectral simulation.

gradually changed as a function of temperature. This spectral change was completely reversible. The ^{1}H-hyperfine parameters were determined by spectral simulation[19] (Figure 3 and Figure S7 in the Supporting Information): The experimental *g* value was constant in the temperature range. Interestingly, $A^{H2,5,8}$ (blue circles) continuously decreases with decreasing temperature, while A^{OMe} (pink circles) continuously increases. As a result, the difference between the observed A^{OMe} at 298 K (+0.0392 mT in Table S1) and the calculated A^{OMe} for the optimized structure of **1**• (+0.0802 mT in Table S1) becomes smaller in the low temperature region (e.g. A^{OMe} = 0.0560 mT at 175 K). The findings suggest that the spin delocalization onto the methoxy groups from the phenalenyl skeleton is enhanced owing to vibronic effects with decreasing temperature. Furthermore, the ESR signal intensity of **1**• decreases with decreasing temperature, thus suggesting the

possible formation of a closed-shell diamagnetic dimer at low temperature, as also seen in TBPLY.[20–22]

The observed temperature dependence of the hfccs of **1**· strongly suggests the occurrence of conformational changes of the methoxy groups. Thus, we calculated $A^{H2,5,8}$, A^{OMe}, and the total energy for **1**· as a function of the dihedral angle between the methoxy group and the phenalenyl π plane (Figure 4). A synchronized rotation of the methoxy groups related by the

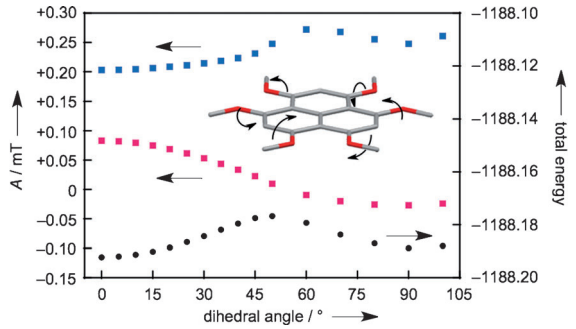

Figure 4. Angular dependence of $A^{H2,5,8}$ (blue squares, left), A^{OMe} (pink squares, left), and the total energy (black circles, right) for **1**· calculated by using the DFT method (UB3LYP/DZVP2). The inset shows the structure of **1**· with the dihedral angle 0°. The six methoxy groups are symmetrically rotated all together in the direction of each arrow from the coplanar state with the dihedral angle 0°.[23] A synchronized rotation of the methoxy groups related by the C_3 symmetry operation was assumed.

C_3 symmetry operation was assumed. The arrows in the inset of Figure 4 represent the rotary direction from the coplanar structure with the dihedral angle = 0°.[23] With increasing the dihedral angle from 0° to 60°, $A^{H2,5,8}$ (blue squares) increases and A^{OMe} (pink squares) decreases. This tendency indicates that the decrease in the π conjugation hinders the spin delocalization onto the methoxy groups from the phenalenyl skeleton. Furthermore, as shown in Figure 4, in the 0–45° region the hfccs follow a trend that is similar to the experimental tendency of $A^{H2,5,8}$ and A^{OMe} seen in Figure 3. Also, Figure 4 shows that the calculated total energy of **1**· (black circles) decreases with decreasing the dihedral angle from 45° to 0°. Therefore, the molecule **1**· in solution at low temperature probably forms a thermodynamically stable planar molecular structure with a smaller dihedral angle, in which the free rotation of the methoxy groups slows down.[24] These results suggest that this type of temperature-dependent conformational change in **1**· gave rise to the temperature-dependent hfcc changes (Figure 3) as well as the difference between the observed (at 298 K) and calculated A^{OMe} (Table S1 in the Supporting Information). In addition, the higher molecular planarity of **1**· at low temperature might enhance an intermolecular π–π interaction, to form closed-shell π-dimeric pairs, as the temperature dependence of the ESR signal intensity suggested (described above).[20–22] Experimental characterization of the dimer structure and the dimerization phenomenon is underway.

The electronic and nuclear spin properties of **1**· attributable to the symmetric molecular structure have been well identified. This encouraged us to search for novel quantum coherence owing to extremely high degeneracy of nuclear spin states; modern classical computers cannot treat such quantum coherence in an exact and numerical manner. The highly symmetric neutral radical **1**· accommodates many equivalent fermions (proton nuclei) that are equivalently connected through a delocalized π spin. In this context, the highly symmetric neutral radical **1**· can be a model for molecular quantum spin simulators (QSSs), which gives quantum coherence of highly degenerate nuclear spin dynamics in solution. Pulse-based time-domain ESR spectroscopy has been applied for **1**· in solution. We modified a Bruker X-band ESP380E spectrometer so that it was controlled by SpecMan4EPR software.[25] In Figures 5 and 6, typical time-domain and FT-ESR spectra of **1**· in degassed toluene (6×10^{-4} M) are shown (see also Figure S10 in the Supporting Information). The free induction decay (FID) in

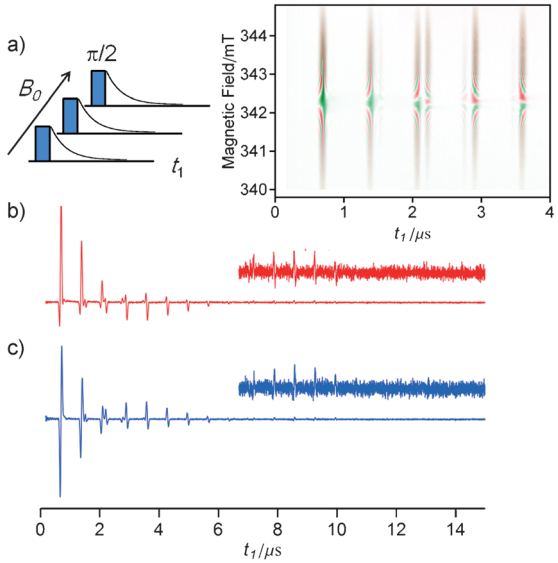

Figure 5. Pulse-based time-domain ESR spectra of **1**· observed in degassed toluene (6×10^{-4} M) at 240 K. a) The FID of the electron spin after a π/2 pulse was observed while the static magnetic field swept. A density plot (right) was constructed by using the two-dimensional field-swept FID spectra. The signal intensities after 1.8 μs were magnified by 3 times for clarity. b, c) The quadrature FID signals, i.e., real and imaginary parts, observed at 342.02 mT are given by red (b) and blue (c) lines, respectively. The microwave frequency used was 9.600450 GHz. The pattern and number of the quadrature signals depend on the ESR resonance field.

Figure 5a (right: time evolution patterns given in the 2D representation) depends on the resonance magnetic field, indicating that quantum spin coherence among the resultant proton nuclear spins of **1**· owing to the high degeneracy is evolved. As expected, the FID signals with very long tails were seen over a 10 μs range (Figure 5b, c). Such long tails are due to both long transverse relaxation time T_2 and extremely high nuclear spin multiplicities arising from the high equivalency of protons, where spin-rotational relaxation is involved. In Figure 6, a 3D plot of two-dimensional FT-ESR spectra at 240 K is given on the right side with spectral

simulation (bottom). The simulated spectra were calculated by using the magnetic parameters of **1**• determined by the cw-ESR/ENDOR spectra and with a home-built simulation program based on density matrix formalism. The density

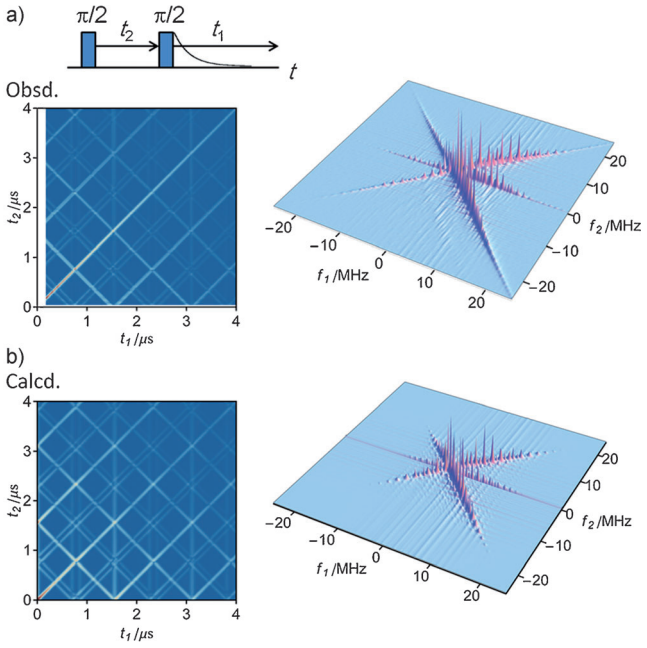

Figure 6. Two-dimensional FT-ESR spectra of **1**• observed in degassed toluene (6×10^{-4} M) at 240 K. An applied pulse sequence for the correlation ESR spectroscopy is given at the top of (a). The observed and calculated density maps of the power spectra are shown on the left in (a) and (b). The simulated spectra on the right in (b) were calculated for $(1-\delta)\pi/2-t_2-(1-\delta)\pi/2-t_1$, where $\delta=0.1$. The time-domain ESR spectra shown in (a) on the left were measured at 342.37 mT in the field-swept ESR spectrum. The microwave frequency used was 9.600505 GHz.

maps of the corresponding power spectra are given on the left of Figure 6. The observed reticular time-domain patterns in Figure 6a (left) show constructive signal phase interference between the unpaired electron and resultant proton nuclear spins. The time profile of the pattern depends on the nuclear features of resultant nuclear spins and interactions among spins involved in the system. The time evolution of the spin magnetization owing to **1**• in solution is reproduced, including signals appearing at zero frequency in the f_2 axis in Figure 6 (right). The zero frequency signals are due to the imperfectness of the actual applied π/2 microwave pulses. Agreement between theory and experiment is not perfect, particularly in the long tail of the diagonal part. This is due to the limit of our computation resource, i.e., the limit of any conventional modern classical computers. The limit only allows us to handle small subspaces among the extremely highly degenerate nuclear spin states, the spin dynamics of which have never explicitly been treated so far to derive quantum coherence. The present quantum coherence among the equivalent nuclear fermions is dominantly electron-spin mediated. Thus, we were forced to neglect spin-rotational interactions and nuclear spin–spin couplings inherently involved in the system. In addition, the present simulation does not include the ^{13}C hyperfine contribution found in the observed spectra. Importantly, the pulse experiments on **1**• show that novel interference patterns arising from spin quantum coherence among many extremely high spin multiplicities composed of the eighteen equivalent fermions (protons) manifest themselves in the time-domain spectra. This appearance allows us to manipulate or store the spectral information that is accumulated in the time-domain signals. Detailed analysis and possible implementation of molecular QSSs are underway, particularly focusing on the analysis of spectral phases appearing in the 1D time-domain spectra (Figure 5). A phase-controlled technique based on time-proportional phase increments (TPPI) is applicable to identify the quantum coherence through multiple quantum transitions among many nuclear spins composed of the eighteen equivalent fermions.[4a,26]

In conclusion, an electronically stabilized phenalenyl radical **1**• with six methoxy groups introduced symmetrically at all the α-carbon atoms has been synthesized, and its novel spin-based quantum nature[27] relevant to spin dynamics of a large number of interacting equivalent fermions in symmetric molecular frames has been studied by the cw- and 2D-COSY-type pulsed-ESR techniques. From a viewpoint of synthetic chemistry, the present study demonstrates that molecular designs utilizing the resonance effect on condensed polycyclic carbon-centered neutral π-radical systems are useful and even promising for the stabilization of the radical species themselves. A salient feature of the stabilized phenalenyl radical **1**• with the methoxy groups introduced in a highly symmetric manner allows us to explore molecular quantum spin simulators for studying a large number of interacting equivalent spins in molecular frames, exemplifying that quantum coherence owing to the extremely high degeneracy of nuclear fermions appears in solution. The coherence arises from synchronized rotational motions of the interacting nuclear spins in the spin-delocalized molecular frame of the phenalenyl skeleton. Studies of nuclear spin–spin couplings in the stabilized phenalenyl radical **1**•, spin-rotational interactions, and their contribution to the spin dynamics are underway, combined with the TPPI experiments on the detection of the multiple quantum transitions.

Received: February 19, 2013
Published online: April 2, 2013

Keywords: density functional calculations · EPR spectroscopy · quantum coherence · radicals

[1] a) A. R. Forrester, J. M. Hay, R. H. Thomson, *Organic Chemistry of Stable Free Radicals*, Academic Press, London, **1968**; b) R. G. Hicks, *Org. Biomol. Chem.* **2007**, *5*, 1321–1338; c) *Stable Radicals: Fundamentals and Applied Aspects of Odd-Electron Compounds* (Ed.: R. G. Hicks), Wiley, Chichester, **2010**.

[2] a) *Magnetic Properties of Organic Materials*, (Ed.: P. M. Lahti), Marcel Dekker, New York, **1999**; b) *Molecular Magnetism* (Eds.: K. Itoh, M. Kinoshita), Kodansha, and Gordon and Breach Science Publishers, Tokyo, **2000**; c) *Magnetism: Molecules to*

Materials, *Vol. I–V* (Eds.: J. S. Miller, M. Drillon), Wiley-VCH, Weinheim, **2001–2005**.

[3] Y. Matsuki, T. Maly, O. Ouari, H. Karoui, F. Le Moigne, E. Rizzato, S. Lyubenova, J. Herzfeld, T. Prisner, P. Tordo, R. G. Griffin, *Angew. Chem.* **2009**, *121*, 5096–5100; *Angew. Chem. Int. Ed.* **2009**, *48*, 4996–5000.

[4] a) K. Sato, S. Nakazawa, R. Rahimi, T. Ise, S. Nishida, T. Yoshino, N. Mori, K. Toyota, D. Shiomi, Y. Yakiyama, Y. Morita, M. Kitagawa, K. Nakasuji, M. Nakahara, H. Hara, P. Carl, P. Höfer, T. Takui, *J. Mater. Chem.* **2009**, *19*, 3739–3754; b) Y. Morita, Y. Yakiyama, S. Nakazawa, T. Murata, T. Ise, D. Hashizume, D. Shiomi, K. Sato, M. Kitagawa, K. Nakasuji, T. Takui, *J. Am. Chem. Soc.* **2010**, *132*, 6944–6946; c) T. Yoshino, S. Nishida, K. Sato, S. Nakazawa, R. D. Rahimi, K, Toyota, D. Shiomi, Y. Morita, M. Kitagawa, T. Takui, *J. Phys. Chem. Lett.* **2011**, *2*, 449–453; d) S. Nakazawa, S. Nishida, T. Ise, T. Yoshino, N. Mori, R. D. Rahimi, K. Sato, Y. Morita, K. Toyota, D. Shiomi, M. Kitagawa, H. Hara, P. Carl, P. Höfer, T. Takui, *Angew. Chem.* **2012**, *124*, 9998–10002; *Angew. Chem. Int. Ed.* **2012**, *51*, 9860–9864.

[5] a) D. H. Reid, *Q. Rev.* **1965**, *19*, 274–302; b) F. Gerson, *Helv. Chim. Acta* **1966**, *49*, 1463–1467.

[6] K. Goto, T. Kubo, K. Yamamoto, K. Nakasuji, K. Sato, D. Shiomi, T. Takui, M. Kubota, T. Kobayashi, K. Yakushi, J. Ouyang, *J. Am. Chem. Soc.* **1999**, *121*, 1619–1620.

[7] a) Y. Morita, T. Ohba, N. Haneda, S. Maki, J. Kawai, K. Hatanaka, K. Sato, D. Shiomi, T. Takui, K. Nakasuji, *J. Am. Chem. Soc.* **2000**, *122*, 4825–4826; b) Y. Morita, T. Aoki, K. Fukui, S. Nakazawa, K. Tamaki, S. Suzuki, A. Fuyuhiro, K. Yamamoto, K. Sato, D. Shiomi, A. Naito, T. Takui, K. Nakasuji, *Angew. Chem.* **2002**, *114*, 1871–1874; *Angew. Chem. Int. Ed.* **2002**, *41*, 1793–1796; c) S. Nishida, Y. Morita, K. Fukui, K. Sato, D. Shiomi, T. Takui, K. Nakasuji, *Angew. Chem.* **2005**, *117*, 7443–7446; *Angew. Chem. Int. Ed.* **2005**, *44*, 7277–7280; d) S. Suzuki, Y. Morita, K. Fukui, K. Sato, D. Shiomi, T. Takui, K. Nakasuji, *J. Am. Chem. Soc.* **2006**, *128*, 2530–2531; e) Y. Morita, S. Suzuki, K. Fukui, S. Nakazawa, H. Kitagawa, H. Okamoto, A. Naito, A. Sekine, Y. Ohashi, M. Shiro, K. Sasaki, D. Shiomi, K. Sato, T. Takui, K. Nakasuji, *Nat. Mater.* **2008**, *7*, 48–51; f) A. Ueda, H. Wasa, S. Suzuki, K. Okada, K. Sato, T. Takui, Y. Morita, *Angew. Chem.* **2012**, *124*, 6795–6799; *Angew. Chem. Int. Ed.* **2012**, *51*, 6691–6695.

[8] P. A. Koutentis, Y. Chen, Y. Cao, T. P. Best, M. E. Itkis, L. Beer, R. T. Oakley, C. P. Brock, R. C. Haddon, *J. Am. Chem. Soc.* **2001**, *123*, 3864–3871.

[9] For overviews of recent phenalenyl chemistry, see: a) "Phenalenyls, Cyclopentadienyls, and Other Carbon-Centered Radicals"Y. Morita, S. Nishida in *Stable Radicals: Fundamentals and Applied Aspects of Odd-Electron Compounds* (Ed.: R. G. Hicks), Wiley, Chichester, **2010**, pp. 81–145; b) Y. Morita, S. Suzuki, K. Sato, T. Takui, *Nat. Chem.* **2011**, *3*, 197–204.

[10] a) K. Nakasuji, M. Yamaguchi, I. Murata, K. Yamaguchi, T. Fueno, H. Ohya-Nishiguchi, T. Sugano, M. Kinoshita, *J. Am. Chem. Soc.* **1989**, *111*, 9265–9267; b) Y. Morita, E. Miyazaki, T. Yokoyama, T. Kubo, E. Mochizuki, Y. Kai, K. Nakasuji, *Synth. Met.* **2003**, *135–136*, 617–618; c) A. Ueda, K. Yoshida, S. Suzuki, K. Fukui, K. Nakasuji, Y. Morita, *J. Phys. Org. Chem.* **2011**, *24*, 952–959; d) T. Murata, E. Miyazaki, T. Yokoyama, K. Nakasuji, Y. Morita, *Cryst. Growth Des.* **2012**, *12*, 804–810.

[11] a) L. Beer, S. K. Mandal, R. W. Reed, R. T. Oakley, F. S. Tham, B. Donnadieu, R. C. Haddon, *Cryst. Growth Des.* **2007**, *7*, 802–809; b) L. Beer, R. W. Reed, C. M. Robertson, R. T. Oakley, F. S. Tham, R. C. Haddon, *Org. Lett.* **2008**, *10*, 3121–3123.

[12] S. Nishida, K. Kariyazono, A. Yamanaka, K. Fukui, K. Sato, T. Takui, K. Nakasuji, Y. Morita, *Chem. Asian J.* **2011**, *6*, 1188–1196.

[13] We recently revealed that tribrominated trioxotriangulene, a phenalenyl-based 25π-conjugated carbon-centered neutral radical, is extremely stable in air in both the solid and solution states, though the radical is sterically little protected. Y. Morita, S. Nishida, T. Murata, M. Moriguchi, A. Ueda, M. Satoh, K. Arifuku, K. Sato, T. Takui, *Nat. Mater.* **2011**, *10*, 947–951.

[14] In addition to the electronic stabilization effect, the introduced six methoxy groups should provide some steric protection effects, although they are less bulky than usual bulky substituents such as *tert*-butyl groups.

[15] Cation salt $\mathbf{1}^{+}\cdot BPh_4^-$ was synthesized according to the literature (Ref. [10c]). We have solved the crystal structure of $\mathbf{1}^{+}\cdot BPh_4^-\cdot H_2O$. For details, see the Supporting Information.

[16] In contrast to **1**$^{\bullet}$, the 1,3,4,9-tetramethoxyphenalenyl radical is reported to gradually decompose to a peropyrene derivative in solution through σ dimerization. See, Ref. [11a].

[17] All DFT calculations were performed with the Gaussian03 program (revision E.01) Gaussian, Inc., Wallingford CT, 2004; the full reference is listed in the Supporting Information. The UB3LYP/DZVP method was applied to the calculations, noting that the DZVP or DZVP2 basis set reasonably reproduces the experimental hyperfine coupling constants of organic open-shell systems. See Ref. [4c].

[18] An electronic effect of the methoxy groups was also examined in terms of the redox properties and the frontier orbital energies of the cation species $\mathbf{1}^{+}$ and $TBPLY^{+}$. For details, see the Supporting Information.

[19] S. Stoll, A. Schweiger, *J. Magn. Reson.* **2006**, *178*, 42–55.

[20] The temperature dependence of the ESR signal intensity of **1**$^{\bullet}$ is shown in the Supporting Information.

[21] TBPLY forms a closed-shell π-dimeric pair in solution at low temperature by the π–π interaction between singly occupied molecular orbitals (SOMOs). D. Small, V. Zaitsev, Y. Jung, S. V. Rosokha, M. Head-Gordon, J. K. Kochi, *J. Am. Chem. Soc.* **2004**, *126*, 13850–13858. See also Ref. [7d].

[22] The possibility of dimer formation was also suggested by solution-phase UV/Vis spectra of the neutral radical **1**$^{\bullet}$. See the Supporting Information.

[23] We understand that there are other rotation modes of the six methoxy groups. To simply evaluate the effect of the dihedral angle change, we have chosen the model with the symmetric rotation in this study.

[24] The temperature dependence of the ESR linewidth of **1**$^{\bullet}$ suggests that the molecular motion of **1**$^{\bullet}$, which includes the free rotation of the methoxy groups, slows at low temperature.

[25] B. Epel, I. Gromov, S. Stoll, A. Schweiger, D. Goldfarb, *Concepts Magn. Reson. Part B* **2005**, *26*, 36–45.

[26] M. Mehring, P. Höfer, A. Grupp, *Phys. Rev. A* **1986**, *33*, 3523–3526.

[27] Very recently, the use of a phenalenyl–metal complex for spintronics and memory storage devices has been reported: K. V. Raman, A. M. Kamerbeek, A. Mukherjee, N. Atodiresei, T. K. Sen, P. Lazić, V. Caciuc, R. Michel, D. Stalke, S. K. Mandal, S. Blügel, M. Münzenberg, J. S. Moodera, *Nature* **2013**, *493*, 509–513.

